

The Effect of Resolution on Scaling Relations and Concavity on Valley Networks on Mars

Peter G. Smith

Department of Resource Analysis, Saint Mary's University of Minnesota, Winona, MN 55987

Keywords: GIS, DEM, Mars, Scaling, Valley Networks, Geomorphology

Abstract

Valley networks have been observed on Mars since the Viking orbiter took photos in 1976-1980. They are interpreted as an erosional record of a warmer, wetter Mars than what currently exists. Scaling relationships have been used to evaluate terrestrial streams and can be used on Mars. Results from these relationships can provide insight into the mechanisms that formed the valley networks. These relationships, when compared to earth data are consistent with immature, precipitation fed valley networks. The range of values calculated may change based on quality of data used. The Mars Orbiter Laser Altimeter (MOLA) created a DEM of the entire planet of Mars at 128/pixel per degree or 460-meter resolution. In this study, this resolution (460-meter) is compared with the High-Resolution Stereo Camera (HRSC) derived DEM at 75 pixels/degree or 150-meter resolution. The results show a difference in the scaling exponents but within an acceptable range. However, when comparing data collected at the same location, measurements are shown to be statistically different.

Introduction

The old surfaces of Mars are covered with evidence of liquid water existing on the surface. Branching channel systems on Mars are known as "Valley Networks." Valley networks are widely interpreted as the preserved erosional record of water flowing over the Martian surface (Milton, 1973).

The existence of valley networks on the surface of Mars is the strongest evidence the surface once was much warmer than current conditions. It is uncertain the duration, intensity, and surface conditions that would form these Valley networks (Penido, Fasset, and Som, 2012).

Mars was formed 4.1 to 3.8 Giga Years Ago (gya) according to Martian meteorites found on earth. Martian time is

divided into 3 major time periods, the Noachian 4.1-3.7 gya, Hesperian 3.7-3.0 gya and the Amazonian 3.0- present (Carr and Head, 2010). Much of the Noachian terrain contains valley networks. Most are a few hundred kilometers long and drain into local lows. Stream profiles are poorly graded and directly follow regional slope (Howard, Moore, and Irwin, 2005).

The goal of this project was to compare the physical relationship parameters of terrestrial fluvial morphology on a Martian valley network using data from the Mars Orbiter Laser Altimeter (MOLA) topographic data and the Thermal Emissions Imaging System (THEMIS) images. Project objectives included comparing MOLA data to data derived from the High-Resolution Stereo Camera (HRSC).

MOLA was one of five instruments aboard the Mars Global Surveyor spacecraft. MOLA collected topography data from 1997 to 2006 about the surface of Mars by using an infrared laser pulsing 10 times a second measuring time between the pulse leaving and arriving back to the orbiter. This craft was designed by NASA and operated for 9 years in orbit around Mars. The mission cost \$154 million to develop and build, \$64 million to launch, and \$20 million a year to operate (Smith, Zuber, Frey, Garvin, Head, Muhleman, and Pettengill, 2001).

The THEMIS instrument was a camera on board the Mars Odyssey orbiter. The THEMIS camera images visible and infrared parts of the electromagnetic spectrum in order to determine the thermal properties of a surface. This orbiter was developed by NASA and is still in operation and has been for over 11 years. This mission cost \$165 million to develop and build, \$53 million to launch, and \$79 million to operate (Christensen, 2004).

The European Space Agency

launched the Mars Express in 2003 with the HRSC aboard. The HRSC instrument is designed to map the structure, topography, morphology and geologic context of the surface of Mars. This mission is still active and has been so for over 9 years. HRSC's mission consists of imaging the Martian surface in stereo and color with resolutions up to 10 m/pixel (Jaumann, Neukum, Behnke, Duxbury, Eichentopf, Flohrer, and Gasselt, 2007).

While the MOLA and THEMIS datasets exist for the entire planet of Mars, the HRSC does not. This limited possible areas to consider for study because the selected area must contain data for both datasets. Also the valley network selected for study needed to have the least amount of post fluvial degradation. Finally, valley networks that contained inter valley network lakes should not be used (Penido *et al.*, 2012).

North of the Hellas basin there is a valley network identified by Hynek, Beach, and Hoke (2010). This valley network is 924,576 meters in length and is located at 63°E and 20°S. This area

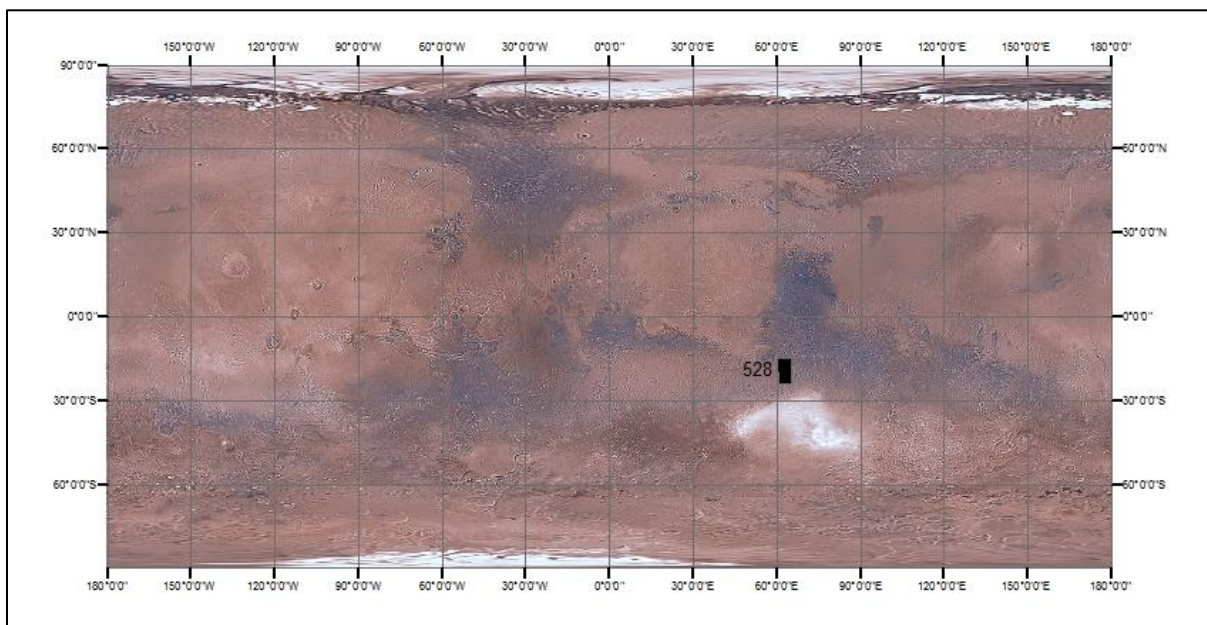


Figure 1. The image footprint for the HRSC orbit number 528, representing the study area highlighted in black.

(Figure 1) is the study area for this research. Penido *et al.* (2012) calculated the scaling relationships on nearby valley networks and these can be used for comparison. Impact craters can affect valley formation; in order to compensate for this, the valley selected post dates the period of heavy bombardment (>3.7 Gya) (Howard, 2007).

Scaling Relations

Terrestrial streams have long been recognized as exhibiting an empirical relationship that relates channel properties such as slope, width, and length to the discharge or drainage area (Hack, 1957; Leopold and Maddock, 1953; Whipple and Tucker, 1999; Leopold and Miller, 1956). These relationships exist as power law functions and have been shown to be true for terrestrial precipitation-fed channel networks. These relationships can be used to compare the different resolution datasets.

Width-Area Scaling

Leopold and Maddock (1953) quantified downstream trends on streams, noticing an increase in width with discharge. The terrestrial value associated is $b \sim 0.5$. The equation relating how channel width (W) scales with discharge (Q) is written as

$$W \propto Q^b.$$

Whipple (2004) suggests a drainage area (A) can be used instead of discharge resulting in an equation that can be rewritten as

$$W \propto A^b.$$

While this equation was designed to be used with channels width instead of

valley width, valley width was used in place of channel width since most the primary channel on the Martian surface cannot be determined (Snyder and Kammer, 2008; Som, Montgomery, and Greenberg, 2009). Also, the difference in acceleration due to gravity on Mars does affect the width of the channel, but not the overall trend as shown by Finnegan, Roe, Montgomery, and Hallet (2005).

Hack's Law

Hacks law is a scaling relationship between the channel length (L) and drainage area (A) (Hack, 1957). This has been shown to be accurate for a full range of perennial and ephemeral terrestrial channels (Montgomery and Diedrich, 1992). The relationship is written as

$$L \propto A^h.$$

Slope-Area Scaling

Streams have long been known to form a concave river profile of the slope decreasing downstream and this has been recognized as a erosional tradeoff between the slope and discharge (Gilbert, 1877). Whipple and Tucker (1999) derived a scaling relationship of river slope to drainage area by proposing that erosion rate is a power function of sheer stress. This has been shown to be true assuming a balance between uplift and incision (Howard, 1994; Howard and Kerby, 1983). Slope(S) relating to drainage area (A) is written as

$$S \propto A^{-\theta}.$$

Theoretically this value should be $\theta = 0.5$ except values of 0.4-0.5 are typically found in active terrestrial streams (Whipple and Tucker, 1999).

Measurements of dry land rivers longitudinal profiles suggest a lack of variability in downstream slope. Positive values of θ are still expected for non-arid channels carved by precipitation-fed flows (Hooke and Mant, 2002).

Langbein Concavity Index

Langbein (1964) proposed an index of concavity independent of drainage area. This is called the Langbein Concavity index (LCI). LCI is based on the shape of the channel's longitudinal profile and is defined as

$$LCI = 2h/H.$$

Where H is the total fall and h is the height difference between the longitudinal profile at mid-distance and a straight line joining the end points of the profile. This method is simple and provides the sign of concavity and has the advantage of not assuming that a surface defined area produces the channel forming runoff. As an example, the Amazon River has a LCI of 1.07 (Knighton, 1998).

Methods

Relevant Data

The data in this study is primarily raster DEM data. First the DEM dataset generated by the MOLA instrument and the DEM created from the HRSC instruments. This is used to determine slope and calculate area drainage.

THEMIS raster images were used to measure the width of the valley network since it has a higher resolution than the MOLA dataset. These measurements will be used for the lower resolution results.

The only shapefile needed is the Valley Network linear created by Hynek *et*

al. (2010). This is an updated map of all known Martian valley networks using all available data. This will be used to help define the valley network length and location. All of these datasets are free and available from the NASA website.

Procedures

In order to use scaling equations, the drainage area, length, width, and slope for the valley network were calculated. In order to do this, the valley networks drainage basin was first defined. The HRSC DEM was imported into ESRI ArcMap and ArcCatalog version 10. Using ArcHydro Tools version 2.0, the basin was defined and set as a mask for the rest of the analysis (Figure 2).

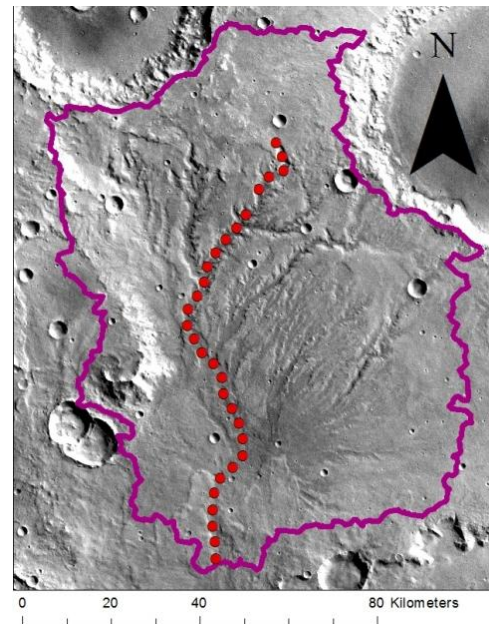


Figure 2. The purple outlines the drainage basin. The red points are locations from which data were collected.

As with most hydrologic analysis before analysis can be run on the DEM, pits need to be filled in order to avoid discontinuous flow patterns (Som *et al.*, 2009). After, the fill flow direction and flow accumulation were calculated. Flow

accumulation was determined by finding the direction of steepest slope from cell to cell keeping track of how many cells flowed into the next downstream cell. Then using the ArcHydro tool ‘Stream Definition’, the flow accumulation the main channel in the valley network was defined. Once the channel was defined, 30 evenly spaced point features were created (Figure 2).

Width measurements were taken at point features using the measure tool using THEMIS (low resolution) and HRSC (High Resolution) images. Drainage area was calculated at each point as well. Using the same procedure used to create the flow accumulation raster for the HRSC data, a second flow accumulation raster was created using the MOLA DEM. The flow accumulation value was changed to drainage area by taking flow accumulation value and multiplying the value by the area of pixel. These methods are based on methods described by (Som *et al.*, 2009; Penito *et al.*, 2012). Slope was calculated using the 3D Analyst tool extension in ArcMap. The linear defining the main channel was converted to a 3D linear and a point profile was created. Slope was calculated on 4 km baseline derived from point profile (Som *et al.*, 2009). The point profile made from the 3D linear was also used to calculate the LCI.

$$LCI = 2h/H.$$

Where H is the total fall and h is the height difference between the longitudinal profile at mid-distance and a straight line joining the end points of the profile (Knighton, 1998). Table 1 displayed the first 5 results collected from the MOLA and THEMIS input data. The length for both datasets remains the same for the both MOLA and HRSC tables. The differences in other measurements lead to difference

exponents and allowed for datasets to be compared. This was done in R and as well as Statistical Package for the Social Sciences (SPSS).

Table 1. MOLA and THEMIS results from the first points .

Location	Drainage Area km ² (A)	Length km (L)	Slope (S)	Width km (W)
1	102.5054	3.72	0.025	0.766
2	182.065	7.44	0.024	0.85
3	216.3764	11.16	0.021	1.3
4	303.6561	14.88	0.025	1.467
5	335.8231	18.6	0.020	1.781

The best-fit parameters and confidence intervals were calculated using the standardized major axis approach to line-fitting (e.g., Warton, Wright, Falster, and Westoby, 2006), and the data analyzed by the SMATR3 package for R (Warton, Duursma, Falster, and Taskinen, 2012). This approach is tough against outliers and allows derivation of significance and confidence intervals. According to Penido *et al.*(2012) this method is preferred over ordinary least squares because this study is only interested in comparing how variables scale against each other, rather than prediction of one from another.

Once the data was entered into R, the scaling exponents were calculated with the following equations using Length (L), Slope (S), Width (W), and Drainage Area (A).

Length-Area Scaling ‘‘Hack’s Law’’

h is the scaling exponent:

$$L=k_1A^h$$

Slope-Area Scaling

θ is the scaling exponent:

$$S=k_2A^{-\theta}$$

Width-area Scaling
 b is the scaling exponent:

$$W = k_3 A^b$$

Results

The valley profiles were plotted using the MOLA and THEMIS (Figures 3-5) and HRSC (Figure 6-8). Results can be seen in Table 2. Significant correlation values were shown for all of the relationships. These results are similar to what is expected for Martian terrain, and within the range of values compiled by Penido *et al.* (2012).

All comparisons reject the null hypothesis of the variables being equal. Results are fairly consistent, when comparing the r squared and p values. The r squared indicates the strength of the relationship; the higher the r squared value, the stronger relationship between variables.

Table 2. Scaling relationships results for both the resolutions of data. All the results are within range calculated by Penido *et al.* (2012).

	MOLA THEMIS	HRSC	Martian Range	Martian Median
Hack's Law $L = k A^h$				
h	0.713	0.631	0.34- 1.92	0.74
R²	0.953	0.948		
p	>2.22E-16	>2.22E-16		
Width-Area $W = k A^b$				
b	0.287	0.248	0.19- 1.68	0.49
R²	0.800	0.883		
p	7.11E-10	9.87E-12		
Slope-Area $S = k A^{-\theta}$				
θ	0.604	0.291	-3.8-2.46	1.08
R²	0.553	0.457		
p	3.77E-06	4.18E-05		
LCI	0.2948	0.026	-3.86- 2.46	0.1

The r square statistic is also known as the coefficient of determination. Hack's r squared was 0.953 for MOLA and 0.948 for HRSC indicating a very strong relationship between the length and drainage area. For Width-Area results for r squared were 0.800 and 0.883 again suggesting a strong relationship. Slope-Area results were 0.553 for the MOLA and 0.457 for HRSC. This shows a weaker relationship between slope and drainage area. All of the p values found were well below 0.01 thus indicating that results were not due to chance.

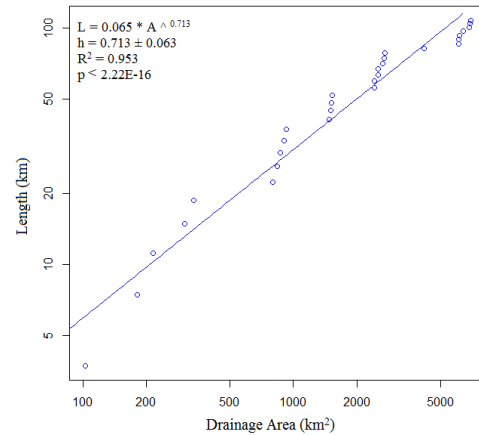


Figure 3. MOLA/THEMIS results for Length-Area (Hack's Law). The p value indicates correlation and a $R^2=0.953$ indicates a strong relationship. The scaling exponent $h=0.713$ is within the expected range.

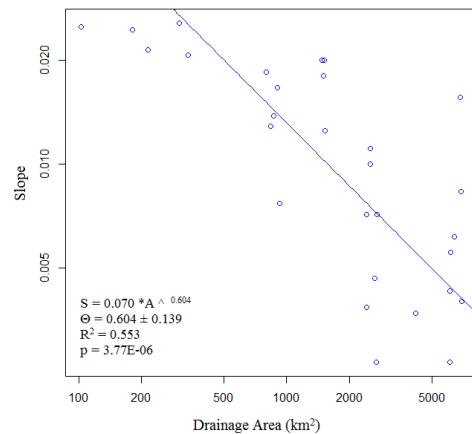


Figure 4. MOLA/THEMIS results for Slope-Area. The p value indicates correlation and a $R^2=0.553$ indicates a weak relationship. The scaling exponent $\theta = 0.604$ is within the expected range.

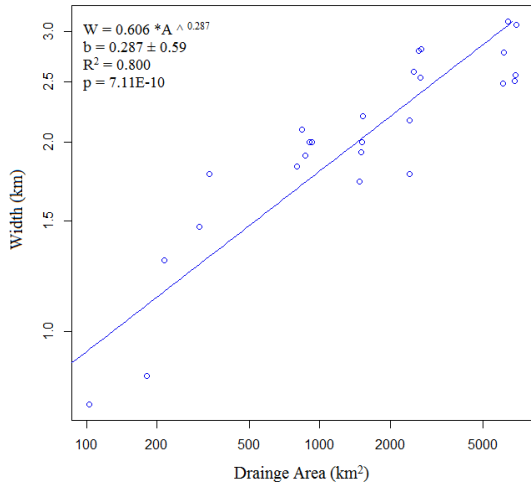


Figure 5. MOLA/THEMIS results for Width-Area. The p value indicates correlation and a $R^2=0.800$ indicates a strong relationship. The scaling exponent $b=0.287$ is within the expected range.

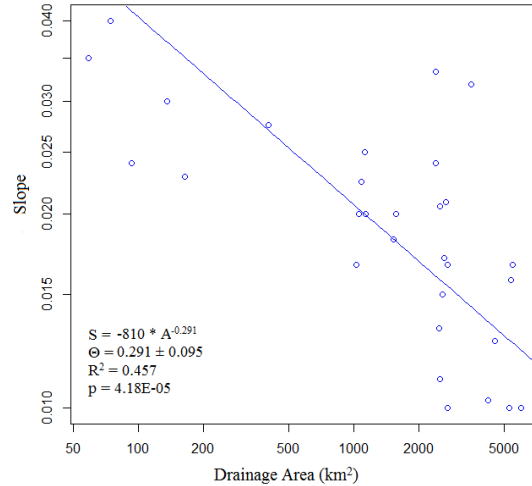


Figure 7. HRSC results for Slope-Area. The p value indicates correlation and a $R^2=0.457$ indicates a weak relationship. The scaling exponent $\theta=0.291$ is within expected range.

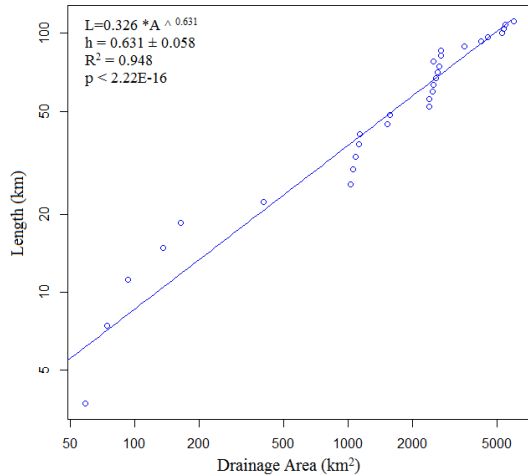


Figure 6. HRSC results for Length-Area (Hack's Law). The p value indicates correlation and a $R^2=0.948$ indicates a strong relationship. The scaling exponent $h=0.613$ is within the expected range.

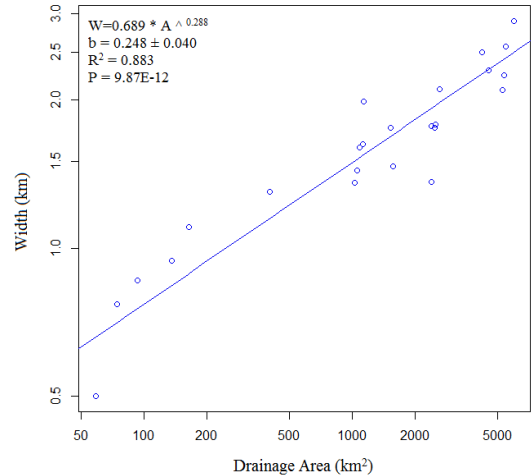


Figure 8. HRSC results for Width-Area. The p value indicates correlation and a $R^2=0.883$ indicates a strong relationship. The scaling exponent $b=0.248$ is within the expected range.

All results fall within the expected values for Martian data and most of the values were very similar. The b values were the most similar with MOLA $b = 0.287$ and HRSC $b = 0.248$ a difference of only 0.039. The largest difference was between the Slope-Area relationship with MOLA $\theta=0.604$ and HRSC $\theta=0.291$ – a difference of 0.313.

Both results yield a positive value for LCI, however the HRSC results were

0.026. According the Penido *et al.* (2012) this value is close enough to 0 to be classified as nearly linear as opposed to the MOLA value of 0.2948 indicating a concave up longitudinal profile.

The Hack's law exponents calculated from the valley network were within the range of other studies, MOLA $h=0.716$ and HRSC $h=0.631$ differ from what is expected for terrestrial data ($h \sim 0.5-0.6$). These results are consistent with work done by Stepenski, Collier,

McGovern, and Clifford, (2004); Som *et al.* (2009); and Penido *et al.* (2012).

Differences between the data sets are not as easily visualized by reading the results in Table 2. All of the scaling relationships use drainage area, a parameter calculated from the flow accumulation. One way to visualize the differences in the compare the results from the stream location derived from ArcHydro using the 'Stream Definition' tool. Figure 9 shows the study area with the streams as defined by ArcHydro. The red lines show stream locations defined from the MOLA data and green from the HRSC. When comparing these results, differences can clearly be seen in the valley network location and flow patterns. This can cause valley network junctions to be missed thus resulting in conflicting values for the drainage area to be used.

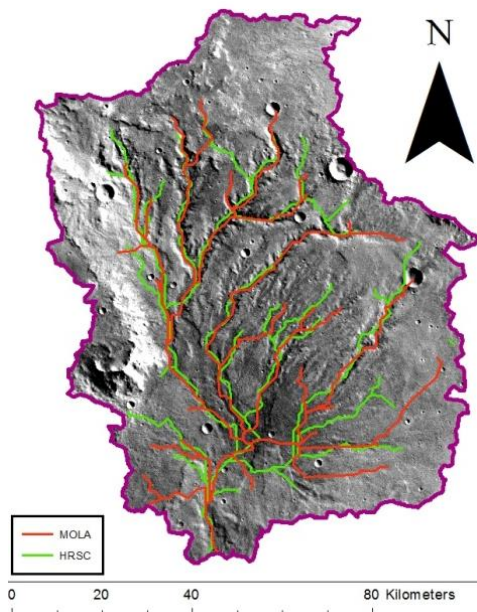


Figure 9. Streams defined by HRSC green and MOLA red.

Since the measurements for the location are not known and cannot be measured via a more accurate method, no dataset can be said to be more accurate than another. The measurements taken

from the MOLA and HRSC datasets were compared to each other on a point by point basis. A descriptive statistics and correlation analysis was done in SPSS to compare the MOLA and HRSC values for width, drainage area, and slope at each point.

Figures 10, 11, and 12 display the different measurements taken at each site. While the measurements are close for some of the points, the best fit lines differ. Since the data are paired a Wilcoxon signed ranks test was used in order to determine if there was a significant difference between the measurements. This test was used for drainage area and slope since these data could be collected at each site.

The width data were compared using a Mann-Whitney test. The results from the Wilcoxon signed ranks test comparing drainage area and slope concluded with 95% confidence that measurements at each point are different for MOLA and HRSC data. For drainage area $Z = -2.335$, $p = 0.010$ and slope $Z = -4.395$, $p < 0.000$. Width was compared using the Mann-Whitney U test resulting with $Z = -2.661$, and $p = 0.008$, Therefore with 95% confidence, width measurements were different for the MOLA and HRSC data.

Regression analysis was also used to compare the data (Table 3). The R squared was used to ascertain data fit to the regression line. This was done to compare the regression relationship between the location, and the measurement taken from the different resolution data. Using a modified t-test, the regression coefficients from the MOLA data were compared to the coefficients of the HRSC. If the slopes of the regression equations were shown to not be equal, no further analysis was needed. If not the elevations of the

regression lines were then compared. Elevation determined if the lines were located at the same location on the graph. If this is, a common equation can be calculated to fit both regression lines.

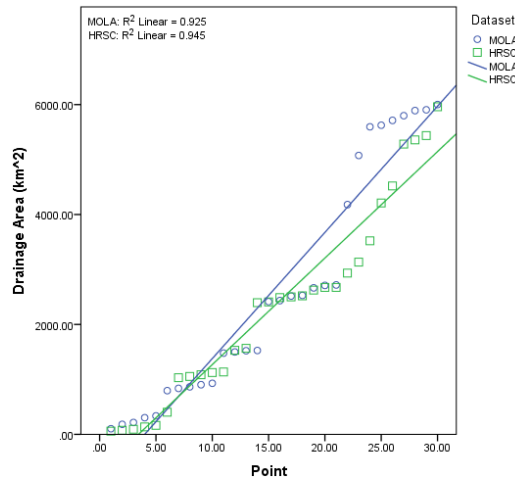


Figure 10. A histogram and best fit line comparing the drainage area measured at each point from the MOLA and HRSC data.

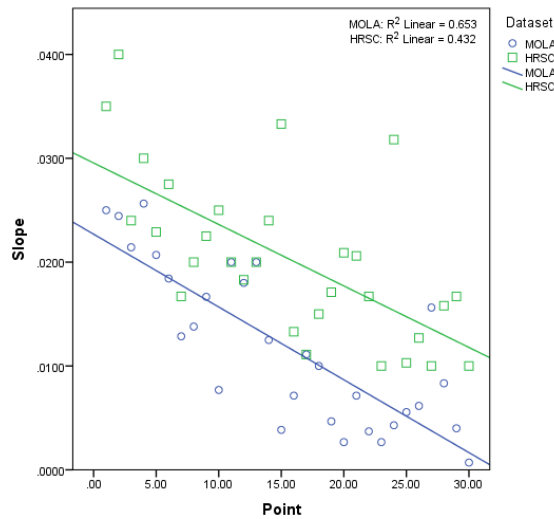


Figure 11. A histogram and best fit line comparing the slope measured at each point from the MOLA and HRSC data.

The t values were compared using a two tailed test at 95% probability. The slope of the drainage area resulted in $t = 2.36$, thus concluding slopes are not the same. Slope and Width Student t values resulted in slopes of the regression equation being equal. Slope $t = 0.68$ and

width $t = 0.22$. Since the regression equation for drainage area was found to not have the same slope, the equation can be concluded with 95% confidence they are statistically different.

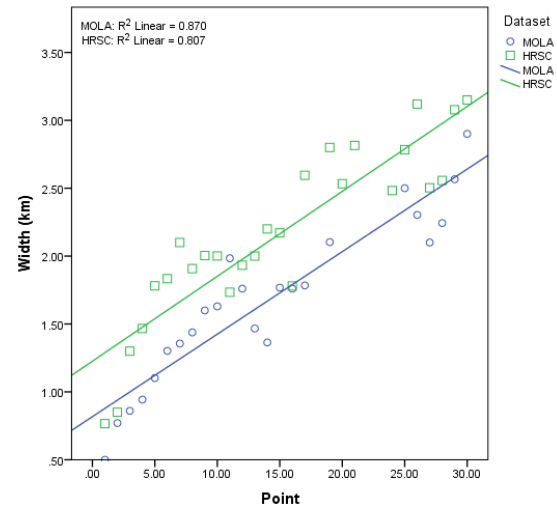


Figure 12. A histogram and best fit line comparing the width measured at each point from the MOLA and HRSC data.

Table 3. The results from the regression analysis on the different measurements and datasets.

	Drainage Area MOLA	Drainage Area HRSC
N	30	30
R ²	0.925	0.945
Adjusted R ²	0.923	0.943
Slope	229.618	193.79
Intercept	-916.872	-667.242
	Slope MOLA	Slope HRSC
N	30	30
R ²	0.653	0.432
Adjusted R ²	0.641	0.412
Slope	-0.001	-0.001
Intercept	0.023	0.03
	Width MOLA	Width HRSC
N	24	27
R ²	0.87	0.807
Adjusted R ²	0.864	0.8
Slope	0.061	0.063
Intercept	0.818	1.226

The elevation of the width and slope were found to not have the same elevation. Slope t was = 6.184 and the width t was = 6.104. Since the regression equation for width and slope were found to not have the same elevation, it can be concluded with 95% confidence that while slopes were statically equal, the lines have different elevations and are statistically different from each other.

The drainage area, slope, and width can also be compared by plotting the MOLA and HRSC against each other on the same graph. With this analysis, an r squared of 0.828 is noted (Figures 13-15).

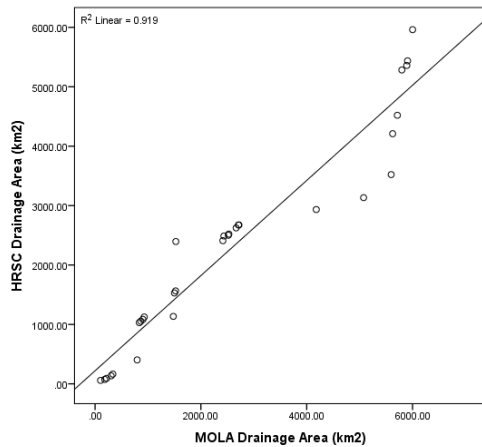


Figure 13. A histogram and best fit line comparing the drainage area measured and plotted with HRSC measurements as Y axis and MOLA as the X axis. The $R^2 = 0.919$.

This indicates MOLA values can be used with a high degree of reliability in predicting what HRSC values might be in areas where HRSC data do not exist. The regression equation for width is $Y = 0.974X + 0.473$. This was used to predict a width value for a point on the HRSC data using a measurement from the MOLA data. For example, at point 19 the MOLA measurement is 2.10 km; as a result, the predicted HRSC measurement would be 2.38 km.

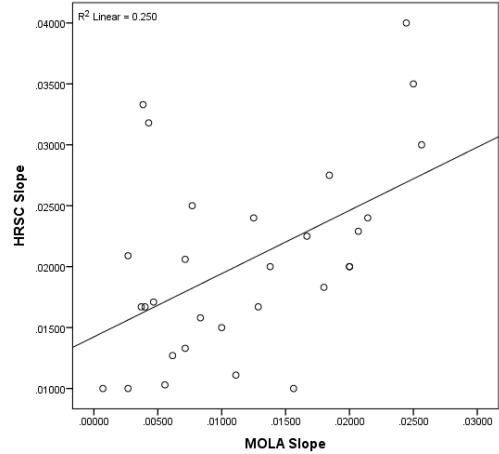


Figure 14. A histogram and best fit line comparing the slope measured and plotted with HRSC measurements as Y axis and MOLA as the X axis. The $R^2 = 0.250$.

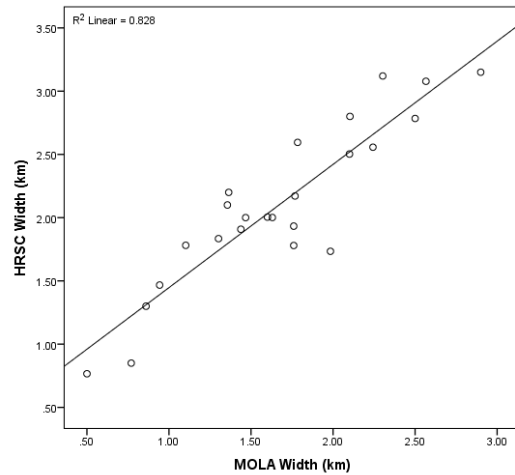


Figure 15. A histogram and best fit line comparing the width measured and plotted with HRSC measurements as Y axis and MOLA as the X axis. The $R^2 = 0.828$.

Conclusion/Discussion

This study used scaling relations to compare measurements taken from two different resolutions of Martian data with the goal of determining if the measurements taken from the different resolution are statistically the same. This was accomplished by comparing the scaling laws exponents. Both resolutions produced scaling relationships that showed correlation and results exponents were

within the accepted values for the Martian surface.

Since true measurements of the Martian surface cannot be measured, measurements taken from the different resolution were compared to each other. The measurements from the HRSC and MOLA at the same point were found to be statistically different from each other. Also, the linear regression equations created from the different resolutions were found to not be the same line. Over 80% of the total variation in the width and drainage area shown in Figures 13 and 15 can be explained by the linear equation. In contrast, only 25% can be explained for slope (Figure 14). In conclusion, since there is not a known value to compare the measurements to, one resolution cannot be said to be more accurate than another, though likely it is the higher resolution HRSC data. It can be said measurements taken at the same location will be statistically different.

Future work

This study only examined one valley network on the Martian surface. There are many other networks where this procedure could be repeated. Also this study examined only two resolutions of Martian data. Some orbiters are collecting DEM data at 1m resolution. Using more resolutions could enhance our understanding of the Martian surface and how resolution affects our conclusions. As mentioned before having known or true measurements gathered on the surface would be ideal.

Acknowledgements

I would like to thank the Saint Mary's University Department of Resource Analysis department staff including Ms.

Greta Bernatz, Dr. Dave McConville, and Mr. John Ebert. Without their teachings, support, and knowledge I would never have completed this program. The experience gained has been invaluable and I am forever grateful and to everyone involved in my graduate work.

References

- Carr, M.H., and Head, J.W. 2010. Geologic History of Mars. *Earth and Planetary Science Letters* 294 (3-4) (June): 185–203. Retrieved on (March 5, 2013) from doi:10.1016/j.epsl.2009.06.042.
- Christensen, P.R. 2004. The Thermal Emissions Imaging System (THEMIS) for the mars 2001 Odyssey Missions. *Space Science Reviews* 110, 85-130, Retrieved on (April 3, 2013) from <http://dx.doi.org/10.1023/B:SPAC.0000021008.16305.94>.
- Finnegan, N.J., Roe, G., Montgomery, D.R., and Hallet, B. 2005. "Controls on the Channel Width of Rivers: Implications for Modeling Fluvial Incision of Bedrock." *Geology* 33 (3) (March 1): 229–232. Retrieved on (March 7, 2013) from doi:10.1130/G21171.1.
- Gilbert, G.K. 1877. Geology of the Henry Mountains. United States Geological Survey. Retrieved on (April 3, 2013) from <http://pubs.er.usgs.gov/publication/70038096>.
- Hack, J.T. 1957. Studies of Longitudinal Stream Profiles in Virginia and Maryland. pp - 294-B. United States Geological Survey. Retrieved on (April 3, 2013) from <http://pubs.er.usgs.gov/publication/pp294B>.
- Hooke, J.M. and Mant, J.M. 2002. Morpho-dynamics of ephemeral streams. In: L.J. Bull and M.J. Kirkby (eds) *Dryland Rivers: Processes and*

- Management in Mediterranean Climates 173- 204.
- Howard, A.D., Moore, J.M., and Irwin, R. P. 2005. A Sedimentary Platform in Margaritifer Sinus, Meridiani Terra, and Arabia. Retrieved on (March 5, 2013) from <http://ntrs.nasa.gov/search.jsp?R=20050170017>.
- Howard, A.D. 1994. A Detachment-limited Model of Drainage Basin Evolution. *Water Resources Research* 30 (7): 2261–2285. Retrieved on (April 3, 2013) from doi:10.1029/94WR00757.
- Howard, A.D. 2007. Simulating the Development of Martian Highland Landscapes through the Interaction of Impact Cratering, Fluvial Erosion, and Variable Hydrologic Forcing. *Geomorphology* 91 (3–4). 332–363. Retrieved on (April 3, 2013) from doi:10.1016/j.geomorph.2007.04.017.
- Howard, A.D., and Kirby, G. 1983. Channel changes in Badlands, Geological Society of America Bulletin. v. 94, p. 739- 752.
- Hynek, B.M., Beach, M., and Hoke, M.R. T. 2010. Updated Global Map of Martian Valley Networks and Implications for Climate and Hydrologic Processes. *Journal of Geophysical Research: Planets* 115 (E9): n/a–n/a. Retrieved on (April 3, 2013) from doi:10.1029/2009JE003548.
- Jaumann, R., Neukum, G., Behnke, T., Duxbury T.C., Eichertopf, K., Flohrer, J., and Gasselt, S.V. 2007. The High-resolution Stereo Camera (HRSC) Experiment on Mars Express: Instrument Aspects and Experiment Conduct from Interplanetary Cruise through the Nominal Mission. *Planetary and Space Science* 55 (7–8) (May): 928–952. Retrieved on (April 3, 2013) from doi:10.1016/j.pss.2006.12.003.
- Knighton, D. 1998. Fluvial Forms and Processes, London. Hodder Education.
- Langbein, W.B., 1964. Profiles of Rivers of Uniform Discharge, USGS Prof. Paper, 501-B, 119–122.
- Leopold, L.B., and Maddock, T. 1953. The Hydraulic Geometry of Stream Channels and Some Physiographic Implications. PP - 252. United States Geological Survey. Retrieved on (April 4, 2013) from <http://pubs.er.usgs.gov/publication/pp252>.
- Leopold, L.B., and Miller, J.P. 1956. Ephemeral Streams; Hydraulic Factors and Their Relation to the Drainage Net. *USGS* 282-A.
- Milton, D.G. 1973. Water and processes of degradation in the Martian Landscape. *J. Geophys. Res.*, 78, 4037–4047.
- Montgomery, D.R., Dietrich, W.E., 1992. Channel initiation and the problem of Landscape scale. *Science* 255, 826–830.
- Penido, J.C., Fassett, C.I., and Som, S.M., 2012. Scaling Relationships and Concavity of Small Valley Networks on Mars. *Planetary and Space Science* 75 (January): 105–116. Retrieved on (March 5, 2013) from doi:10.1016/j.pss.2012.09.009.
- Smith, D.E., Zuber, M.T., Frey, H.V., Garvin, J.B., Head, J.W., Muhleman, D. O., and Pettengill, G.H. 2001. Mars Orbiter Laser Altimeter: Experiment Summary after the First Year of Global Mapping of Mars. *Journal of Geophysical Research: Planets* 106 (E10): 23689–23722. Retrieved on (April 3, 2013) from doi:10.1029/2000JE001364.
- Snyder, N.P., Kammer, L.L. 2008. Dynamic adjustments in channel width in response to a forced diversion: Gower Gulch, Death Valley National Park, California. *Geology* 36, 187–190.
- Som, S.M., Montgomery, D.R., and Greenberg, H.R. 2009. Scaling Relations for Large Martian Valleys. *Journal of Geophysical Research: Planets* 114 (E2):

- Retrieved on (March 5, 2013) from doi:
10.1029/2008JE003132.
- Stepinski, T.F., Collier, M.L., McGovern,
P. J., and Clifford, S. M. 2004. Martian
Geomorphology from Fractal Analysis of
Drainage Networks. *Journal of
Geophysical Research: Planets* 109 (E2):
Retrieved on (March 15, 2013) from doi:
10.1029/2003JE002098.
- Warton, D.I., Wright, I.J., Falster, D.S.,
Westoby, M., 2006. Bivariate line-fitting
methods for allometry. *Biological
Reviews* 81, 259-291.
- Warton, D.I., Duursma, R.A., Falster, D.
R., and Taskinen, S. 2012. Smatr 3– an R
Package for Estimation and Inference
About Allometric Lines. *Methods in
Ecology and Evolution* 3 (2): 257–259.
Retrieved on (April 17, 2013) from doi:
10.1111/j.2041-210X.2011.00153.x.
- Whipple, K.X. 2004. Bedrock Rivers and
the Geomorphology of Active Orogens.
*Annual Review of Earth and Planetary
Sciences* 32 (1): 151–185. Retrieved on
(April 5, 2013) from doi:10.1146/
annurev.earth.32.101802.120356.
- Whipple, K.X., and Tucker, G.E. 1999.
Dynamics of the Stream-power River
Incision Model: Implications for Height
Limits of Mountain Ranges, Landscape
Response Timescales, and Research
Needs. *Journal of Geophysical
Research: Solid Earth* 104 (B8): 17661–
17674. Retrieved on (April 5, 2013) from
doi:10.1029/1999JB900120.